Plasmonics (2011) 6:681–687
DOI 10.1007/s11468-011-9251-2

Remote Excitation Polarization-Dependent Surface Photochemical Reaction by Plasmonic Waveguide

Mengtao Sun · Yanxue Hou · Zhipeng Li · Liwei Liu · Hongxing Xu

Received: 24 March 2011 / Accepted: 5 July 2011 / Published online: 2 August 2011

Abstract For the first time, we report remote excitation polarization-dependent surface photochemical reaction by plasmonic waveguide. Remote excitation polarization-dependent surface-enhanced Raman scattering (SERS) spectra indicate a surface photochemical reaction that p-aminothiophenol is converted to p,p′-dimercaptoazobenzene (DMAB) induced by the plasmonic waveguide. Surface plasmon polaritons generated at the end of a silver nanowire can propagate efficiently along the nanowire, and be coupled by nanoparticles near the nanowire as a nanoantenna. Massive electromagnetic enhancement is generated in the nanogap between the nanowire and the nanoparticles. The remote excitation polarization-dependent SERS spectra can be obtained experimentally in the nanogaps; furthermore, the remote excitation polarization-dependent SERS spectra of DMAB reveal the occurrence of this surface catalytic reaction. Theoretical simulations using finite-difference time-domain methods strongly support our experimental results.

Keywords Remote excitation · Polarization-dependent · Surface photochemical reaction · Plasmonic waveguide

M. Sun (✉) · Y. Hou · Z. Li · H. Xu
Beijing National Laboratory for Condensed Matter Physics, Institute of Physics, Chinese Academy of Sciences, P.O. Box 603–146, Beijing 100190, People's Republic of China
e-mail: mtsun@aphy.iphy.ac.cn

Y. Hou
College of Science, Yanshan University, Qinhuangdao 066004, China

Z. Li
Beijing Key Laboratory of Nano-Photonics and Nano-Structure (NPNS), Department of Physics, Capital Normal University, Beijing 100037, People's Republic of China

L. Liu
Suzhou Institute of Nano-Tech and Nano-Bionics, Chinese Academy of Sciences, Suzhou 215125, People's Republic of China

H. Xu
Division of Solid State Physics, Lund University, Lund 22100, Sweden

Introduction

Surface-enhanced Raman scattering (SERS) is widely used in chemistry, biology, physics, heterogeneous catalysis, and material science, because of its extremely high surface sensitivity and powerful applications in fingerprint vibrational spectroscopy in qualitative and quantitative analysis, even at the level of single molecules [1–8]. The electromagnetic enhancement and chemical enhancement mechanisms are generally believed to be mechanisms for SERS [1–5]. The former is caused by local surface plasmon polaritons (SPPs), [1–5] which usually enhance the Raman spectrum over a large frequency range, and the latter is due to changes in the electronic structure of molecule adsorbed on metal surfaces, whereby some Raman peaks undergo enormous selective enhancement [9–12]. Chemical enhancement is typically explained by the charge-transfer (CT) mechanism.

SERS of 4-aminothiophenol (PATP) adsorbed on different metal surfaces has been extensively studied experimentally [13–21]. Strong a_1 and b_2 modes dominate the SERS spectra of PATP. These selective enhancements of b_2 modes were ascribed to the effect of chemical enhancement [13–16]. Recent experimental and theoretical studies revealed that PATP is converted to p,p′-dimercaptoazobenzene (DMAB) by catalytic coupling reactions on silver nanoparticles [17–21], and the so called b_2 vibrational mode of

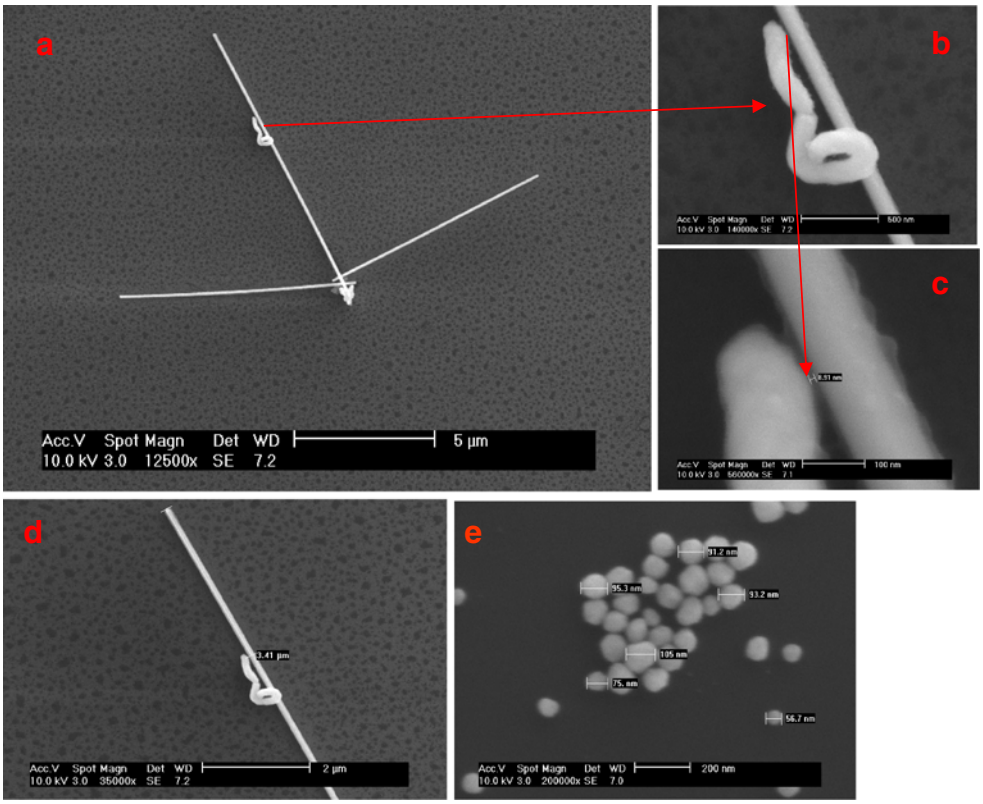

Fig. 1 **a** The SEM imaging of our system, **b–d** are the enlarged **a**

PATP is the symmetric Ag mode of DMAB [17]. In all the above SERS experiments, the incident light is focused onto the SERS active spots on the nanostructure, and the emitted Raman light is detected from the same spots. While this geometry is easy to perform on a substrate, such an approach would not be feasible in many applications, for example, in living systems, where the higher power incident laser light might cause cell destruction or induce a chemical modification of the analyte [22].

SPPs can propagate along metal nanowires, which allow the transfer of light over micrometer distances through structures with sub-diffraction limited diameters [23]. This could lead to miniaturized photonics and help realize high-resolution microscopy/spectroscopy [24]. Recently, remote excitation SERS by propagating SPPs has been investigated experimentally [22–25]. This novel high-sensitive technique can also avoid sample damage from the laser, which may be very useful in special samples such as intercellular molecules of a living cell [25]. This novel high-sensitive technique (remote SERS sensor) can extend conventional local photochemical reactions by nanoparticles to remotely detect surface photochemical reactions in less accessible geometries.

In this communication, we report experimentally and theoretically the remote excitation polarization-dependent

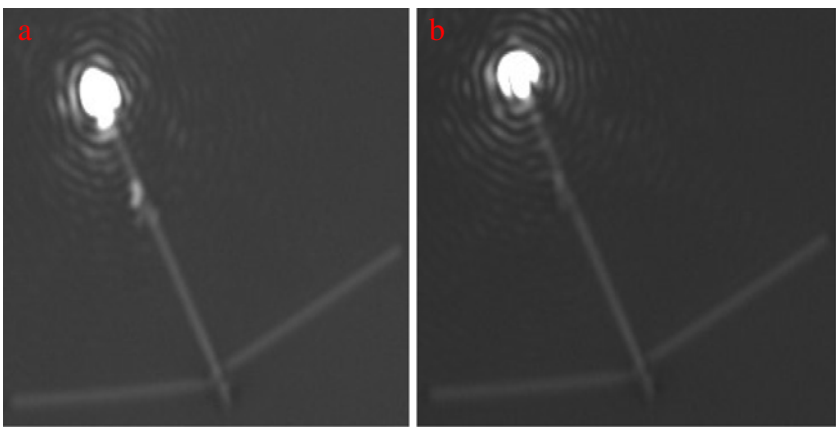

Fig. 2 **a**, **b** The optical images of SPPs propagating along the nanowire, where the polarization of the laser is parallel and perpendicular to the nanowire, respectively

surface photochemical reaction by using a plasmonic waveguide. Firstly, the SPPs propagate efficiently along Ag single-crystalline nanowires, when the incident light radiates on one end of a silver nanowire, where the polarazition of incident laser is parallel to the nanowire. Secondly, the propagating SPPs can be coupled with the nanoparticle antenna in the nanogaps between the nanowire and the nanoparticles. Thirdly, the remote excitation polarization-dependent SERS spectrum is obtained experimentally near the nanogap. Lastly, the SERS spectra reveal that PATP is converted to DMAB by surface catalytic reactions induced by the plasmonic waveguide.

Experimental

The Ag single-crystalline nanowires were prepared by chemical fabrication [26]. To synthesize the Ag nanoparticals, 167 mL poly (vinylpyrrolidone) (PVP, MW=30,000)

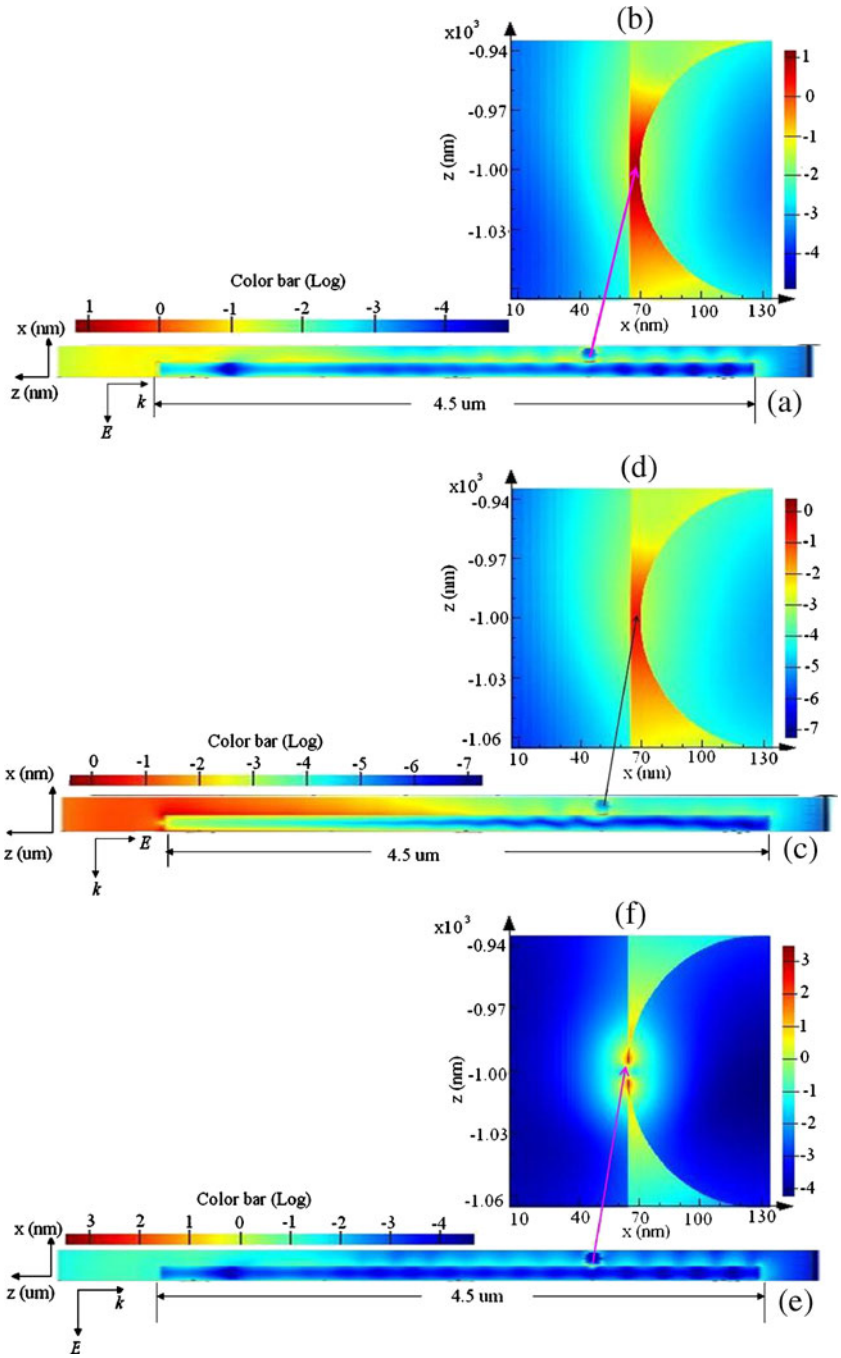

Fig. 3 Simulated Propagating SPPs and near field distribution of the electromagnetic field near the gap between nanowire and nanoparticle. **a** the distance of gap is 5 nm, **b** is the enlarged **a** near the gap; **c** the distance of gap is 5nm, **d** is the enlarged **c** near the gap; **e** the distance of gap is 0 nm, **f** is the enlarged **f** near the gap, in **a**, **b**, **e** and **f** the polarization of laser is parallel to the naniwire, and **c** and **d** the polarization of laser is perpendicular to the nanowire. The *color bar* is in logarithmic scale

was dissolved into 15 mL ethylene glycol (EG) solution under continuous magnetic stirring. Then 0.2 mL $AgNO_3$ aqueous solution (1.5 M) was added. The reaction mixture was kept at 70 °C for 0.5 h in an oil bath, and warmed to 150 °C for 1.5 h. The product was diluted with ethanol and centrifuged four times to remove EG and PVP. The final Ag nanoparticles were mixed with PATP ethanol solution (0.04 M) for 24 h, and were diluted with ethanol.

The Ag nanowires were dropped on the SiO_2 substrate first, and then the mixture of Ag nanoparticles and PATP was dropped. Figure 1a shows a scanning electron microscopy (SEM) imaging of nanowires system. Figure 1b–c are enlarged images of Fig. 1a. Figure 1b shows that the aggregated mixture of PATP and nanoparticles is closed to the nanowire. Figure 1c shows that the efficient detecting distance is about 0–9 nm. Figure 1d shows that the distance between the end of the nanowire and the nanogap is about 3.4 μm. Figure 1e is the SEM image of the nanoparticles.

Bright field images are obtained using Leica microscopy equipment in the confocal Raman spectroscopic system (Renishaw, inVia) through an objective of ×100 with a numerical aperture of 0.85, which is the same objective used for all Raman measurements. The optical image was recorded by a TE-cooled CCD detector equipped on the microscope. The 632.8-nm laser (He–Ne laser) radiates on one end of the silver nanowire. A λ/2 plate corresponding to 632.8 nm laser was used to rotate the polarization of the incident laser. The Raman signal is integrated four times using 1 min, and the laser powder is about 7 mW. For comparison, the SERS spectrum of PATP in Ag sol is also measured.

Theoretical

To understand the propagating SPPs along the Ag nanowire and the coupling effect of electromagnetic field distribution between the nanowire and the nanoparticles, theoretical simulations with the finite-difference time-domain (FDTD) method [27] were done using FDTD Solutions software [28]. We performed the simulation using one 4.5-μm long Ag nanowire with a 130-nm diameter. The nanoparticle (diameter 130 nm) is set at the point that SPPs propagate 3.4 μm (the experimental distance, see Fig. 1d), and the distance between the nanowire and the nanoparticle is set at 5 nm. A polarized Gaussian beam (beam waist is 632.8 nm) was simulated as the excitation source. The permittivity of Ag at 632.8 nm was taken from reference [29].

Results and Discussion

The optical images of nanowires can be seen from Fig. 2, when the laser radiates on one end of the silver nanowire with the parallel and perpendicular polarizations of the laser

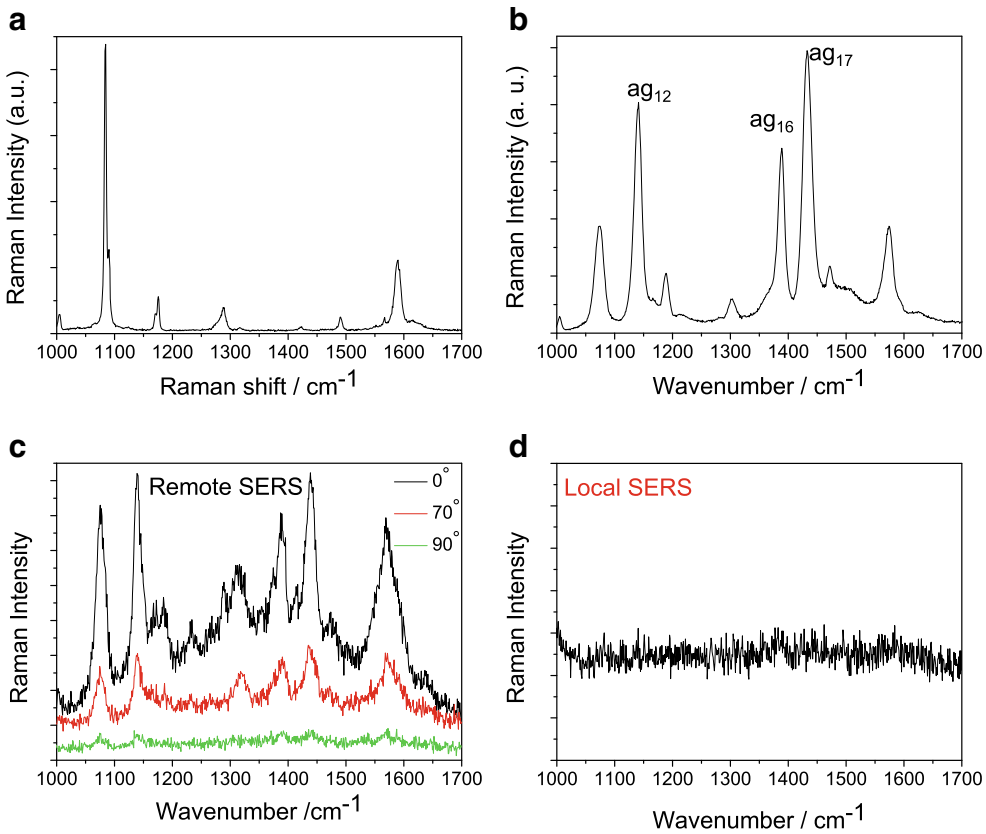

Fig. 4 **a** Normal Raman spectrum of PATP, **b** SERS spectrum of PATP in Ag sol, **c** Remote SERS spectra of DMAB with different angles between polarization of the laser and the nanowire, and **d** the local SERS signal at the end of the nanowire, where the end of the nanowire means the laser radiated point in Fig. 2

to the nanowire, respectively. Figure 2a is the optical image, where the polarization of the laser is parallel to the nanowire. Near the gap between the nanowire and the nanoparticles, one light point can be clearly observed, which is due to the propagating SPPs coupled to the nanoparticle antenna in the aggregated PATP. So, the SPPs can efficiently propagate along the nanowire when the polarization of the laser is parallel to the nanowire, and the propagating SPPs can be coupled to other nanoparticle antennas. Figure 2b is the optical image, where the polarization of the laser is perpendicular to the nanowire. Near the nanoparticles, no light points can be clearly observed. So, the SPPs cannot propagate efficiently along the nanowire when the polarization of the laser is perpendicular to the nanowire.

To better understand the polarization-dependent propagating SPPs along the Ag nanowire and the coupling of electromagnetic field enhancement between the nanowire and the nanoparticles, theoretical simulations were done with the FDTD method. Figure 3a reveals that when the polarization of laser is parallel to the nanowire, the SPPs can be efficiently propagated along the nanowire, and the electromagnetic enhancement $|M|^2$ in the gap between the nanowire and the nanoparticle is about 2.3×10^2 times, where $|M|^2=-E_{local}/E_0|^2$, and the E_{local} and E_0 are the local and incident electric fields, respectively. Figure 3b is the enlarged Fig. 3a near the nanogap between the nanowire and the nanoparticle. Figure 3c–d reveal that when the polarization of the laser is perpendicular to the nanowire, the SPPs cannot be efficiently propagated along the nanowire, the intensity of SPP is decays to 40% in the gap between the nanowire and the nanoparticle and the electromagnetic enhancement $|M|^2=0.16$. One nanoparticle (distance of the gap is 5 nm) is considered in our calculations while there are quite many nanoparticles in the aggregated PATP, and some nanoparticles are closer than the distance in our calculations. So, the experimentally electromagnetic enhancement should be much higher. For the polarization of the laser is parallel to the nanowires when the distance of the gap is 2 nm, the electromagnetic enhancement is about 1.4×10^4 times; furthermore, when the distance of the gap is 0 nm, the electromagnetic enhancement is about 1.0×10^7 times (see Fig. 3e–f).

The normal Raman scattering of PATP in ethanol can be seen from Fig. 4a. We also measured the local SERS spectrum of 4PATP in the Ag sol (see Fig. 4b), and there are three additional strongly enhanced Raman peaks for Ag_{12}, Ag_{16}, and Ag_{17} vibrational modes, which revealed that PATP is converted to DMAB by surface photochemical reactions [17]. The Ag_{17} mode in Fig. 4b is the −N=N- stretching vibrational mode [17]. Note that Fig. 4a–b are the local SERS spectra, where the incident light is focused onto the SERS active spots on the nanostructure and the emitted Raman light is directed from the same spots. To extend this conventional local photochemical reaction (by nanoparticales) to remotely detect surface photochemical reaction by the plasmonic waveguide, we measured the remote excitation SERS induced by the plasmonic waveguide.

The measured remote excitation polarization-dependent SERS spectra induced by the plasmonic waveguide can be seen from Fig. 4c. The three additional strongly enhanced Raman peaks revealed that PATP is converted to DMAB by surface photochemical reactions. So, plasmon enhancements play an important role on the remote surface photochemical reaction, since there is no directly laser radiation on the collection spot of the SERS spectra. In our

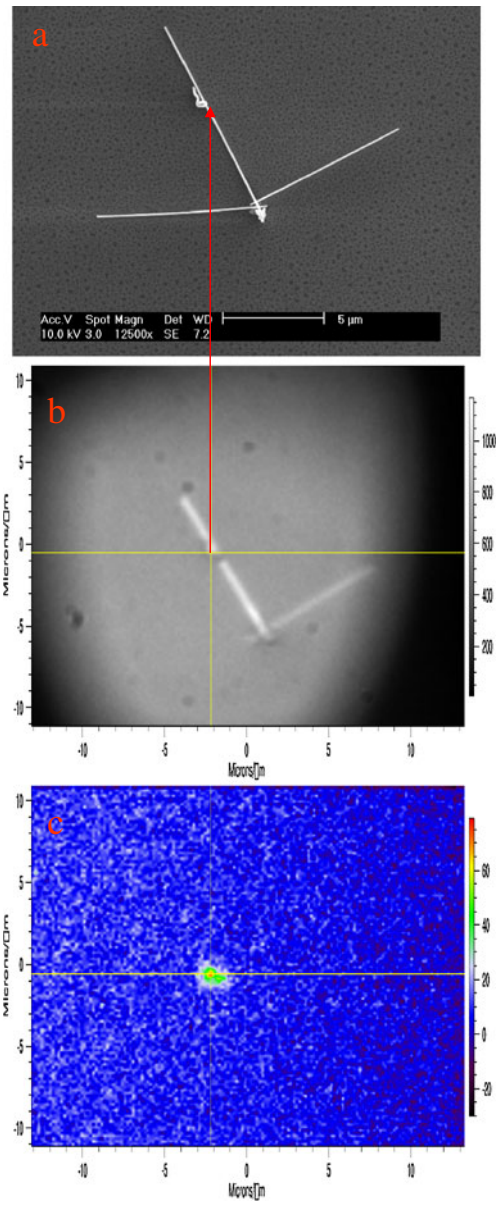

Fig. 5 **a** The SEM image of our system, **b** the optical image of our system, and **c** the remote Raman peak of the Ag_{17} vibrational mode of DMAB

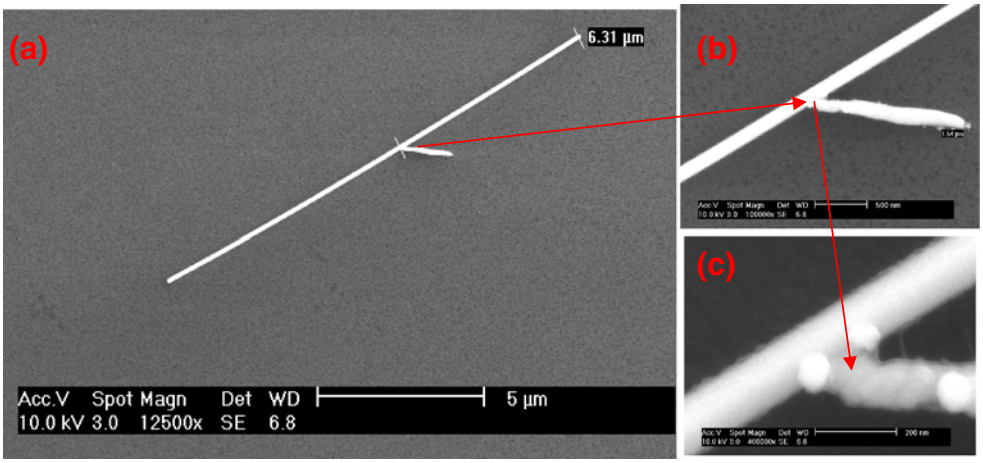

Fig. 6 **a** The SEM image of our system, **b**–**d** are the enlarged **a**

previous study, the influence of the incident polarization on propagating SPPs to the remote SERS is also obtained experimentally and verified by theoretical simulations with the FDTD method [25]. So, polarization-dependent SERS spectra in Fig. 4c reveal that the SERS signals are strongly dependent on the surface plasmon enhancement. When the angle of polarization is increased, the surface plasmon enhancement is decreased, and then the SERS signals are decreased correspondingly. Note that in our experiment, we firstly measured the remote SERS for the case of 0°, and for the case, the strongest intensity of SERS spectra is obtained, which is direct evidence for remote-excitation surface photochemical reactions. For other polarization angles, we considered that the measured Raman signal is directly from DMAB, since the PATP has been catalyzed for the first time measured at the angle 0°. The reason that we measured the Raman signal at different polarization angles is that we demonstrated that the strongest signals can be obtained for the polarization angle 0°.

To clarify the remote excitation polarization-dependent SERS spectra are not the propagating SERS spectrum excited at the end of the nanowire, we also measured the local SERS signal at the end of the nanowire (see Fig. 4d), where the end of the nanowire means the laser radiated point in Fig. 2. It is found that there is no SERS signal. Figure 4d revealed that there is no PATP at the end of nanowire, so the SERS signal measured at remote (see Fig. 4c) cannot be the propagating SERS signal along plasmonic waveguide, and is the SERS signals at remote excited by the plasmonic waveguide.

To further clarify the remote excitation SERS spectrum, we measured the Raman peak of Ag_{17} vibrational mode in the areas that can be observed by the objective (see Fig. 5). Figure 5a is the SEM imaging of our studied system, Fig. 5b is the studied system radiated by bright light, and Fig. 5c is the intensity of Raman peak of Ag_{17} of DMAB in the observed areas, respectively. Figure 5c provides directly experimental evidence for remote excitation surface photochemical reaction of PATP to DMAB by plasmonic waveguide. Figure 5c also reveals that the collected remote excitation SERS is not propagated SERS spectrum (from the endpoint of nanowire) with the plasmonic waveguide.

To provide more clear evidence for the aggregated mixture of PATP and nanoparticles near the nanowire in Fig. 6a–c, another nanowire–nanoparticle system is shown (see Fig. 6). Figure 6c shows that there are two nanoparticles that are closely connected to the nanowire, and the distance between the nanowire and the third nanoparticle is about 200 nm.

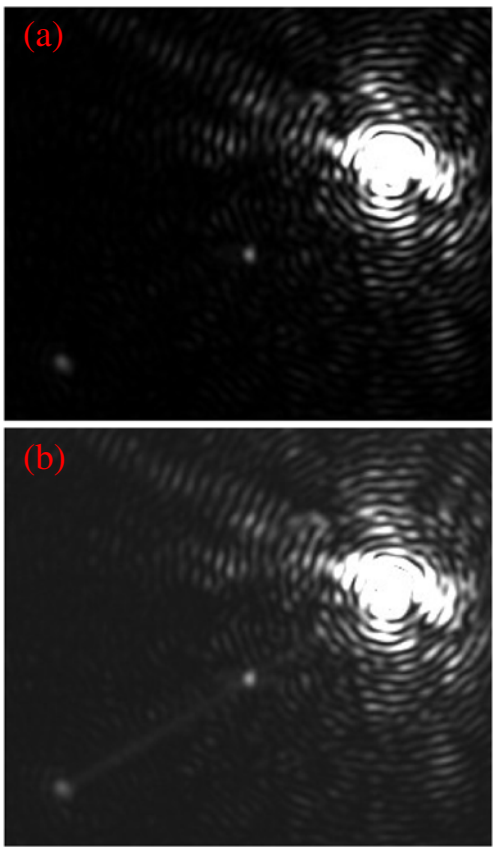

Fig. 7 **a**, **b** are the optical images of SPPs propagating along nanowire, where the polarization of laser is parallel to the nanowire

Figure 7a–b reveal optical properties that the SPPs propagate along the nanowire, when the polarization of the laser is parallel to the nanowire. The plasmonic waveguide can still propagate along the nanowire to the end of the nanowire if the nanoparticle antenna is not very strong.

It is noted that the laser-induced heating effect cannot be ruled out completely, while which is not very important for remote excitation surface catalysis reaction by plasmonic waveguide, since after propagating of plasmonic waveguide along nanowire about several micrometers, it is decayed to vanished small.

Conclusion

Experimental and theoretical evidence revealed that polarization-dependent surface photochemical reactions can occur with the plasmonic waveguide. The remote excitation polarization-dependent SERS signals are strongly dependent on the polarization angles. When the polarization of the laser is parallel to the nanowire, the Raman signals are strongest. This novel highly-sensitive technique can lead to miniaturized photonics and help us realize high-resolution SERS spectra for remote surface catalytic reactions.

Acknowledgments This work was supported by the National Natural Science Foundation of China (grant nos. 90923003, 10874234, 20703064, and 10904171). We thank Dr. Steven L. Suib for helpful suggestions.

References

1. Metiu H, Dos P (1984) Annu Rev Phys Chem 35:507
2. Moskovits M (1985) Rev Mod Phys 57:783
3. Kneipp K, Kneipp H, Itzkan I, Dasari RR, Feld MS (1999) Chem Rev 99:2957
4. Li JF, Huang YF, Ding Y, Yang ZL, Li SB, Zhou XS, Fan FR, Zhang W, Zhou ZY, Wu DY, Ren B, Wang ZL, Tian ZQ (2010) Nature 464:392
5. Steidtner J, Pettinger B (2008) Phys Rev Lett 100:236101
6. Mestl G, Srinivasan TKK (1998) Catalysis Reviews, Science and Engineering 40:451
7. Mestl G (2000) J Mol Catal Chem 158:45
8. Knozinger H, Mestl G (1999) Top Catal 8:45
9. Lombardi JR, Birke RL (2008) J Phys Chem C 112:5605
10. Sun MT, Liu SS, Chen MD, Xu HX (2009) J Raman Spectrosc 40:137
11. Zhao LL, Jensen L, Schatz GC (2006) J Am Chem Soc 128:2911
12. Otto A, Mrozek I, Grabhorn H, Akeman W (1992) J Phys Condens Matter 4:1143
13. Osawa M, Matsuda N, Yoshii K, Uchida I (1994) J Phys Chem 98:12702
14. Gibson JW, Johnson BR (2006) J Chem Phys 124:064701
15. Zhou Q, Li XW, Fan Q, Zhang XX, Zheng JW (2006) Angew Chem Int Ed 45:3970
16. Toderas F, Baia M, Baia L, Astilean S (2007) Nanotechnology 18:255702
17. Fang YR, Li YZ, Xu HX, Sun MT (2010) Langmuir 26:7737
18. Huang YF, Zhu HP, Liu GK, Wu DY, Ren B, Tian ZQ (2010) J Am Chem Soc 132:9244
19. Huang Y, Fang Y, Yang Z, Sun MT (2010) J Phys Chem C 114:18263
20. Canpean V, Iosin M, Astilean S (2010) Chem Phys Lett 500:277
21. Wu DY, Zhao LB, Liu, XM Huang R, Huang YF, Ren B, Tian ZQ (2011) Chem Comm 47:2520
22. Fang YR, Li ZP, Huang YZ, Zhang SP, Nordlander P, Halas NJ, Xu HX (2010) Nano Lett 10:1950
23. Dickson RM, Lyon LA (2000) J Phys Chem B 104:6095
24. Hutchison JA, Centeno SP, Odaka H, Fukumura H, Hofkens J, Uji-i H (2009) Nano Lett 9:995
25. Huang Y, Fang Y, Sun MT (2011) J Phys Chem C 115:3558
26. Sun Y, Xia YN (2002) Adv Mater 14:833
27. Kunz KS, Luebber RJ (1993) The finite difference time domain method for electromagnetic. CRC, Cleveland
28. FDTD solutions, version 7.5; Lumerical Solutions, Inc. Vancounver, British Columbia, Canada, 2009.
29. Palik ED (1985) Handbook of optical constants of solids. Academic, New York